Original Article

Secreted matrix metalloproteinase-14 is a predictor for antifibrotic effect of IC-2-engineered mesenchymal stem cell sheets on liver fibrosis in mice

Kenji Fukushima [a], Noriko Itaba [b], Yohei Kono [b], Shizuma Okazaki [b], Shinpei Enokida [c], Naomi Kuranobu [a], Jun Murakami [a], Makoto Enokida [c], Hideki Nagashima [c], Susumu Kanzaki [a, d], Noriyuki Namba [a], Goshi Shiota [b, *]

[a] Division of Pediatrics and Perinatology, Department of Multidisciplinary Internal Medicine, School of Medicine, Faculty of Medicine, Tottori University, 86 Nishi-cho, Yonago, Tottori, 683-8504, Japan
[b] Division of Medical Genetics and Regenerative Medicine, Department of Genomic Medicine and Regenerative Therapy, School of Medicine, Faculty of Medicine, Tottori University, 86 Nishi-cho, Yonago, Tottori, 683-8503, Japan
[c] Division of Orthopedic Surgery, Department of Sensory and Motor Organs, School of Medicine, Faculty of Medicine, Tottori University, Yonago, 683-8504, Japan
[d] Asahigawaso Rehabilitation & Medical Center, Okayama, 703-8555, Japan

ARTICLE INFO

ABSTRACT

Introduction: Transplantation of IC-2-engineered bone marrow-derived mesenchymal stem cell (BM-MSC) sheets (IC-2 sheets) was previously reported to potentially reduce liver fibrosis.
Methods: This study prepared IC-2-engineered cell sheets from multiple lots of BM-MSCs and examined the therapeutic effects of these cell sheets on liver fibrosis induced by carbon tetrachloride in mice. The predictive factors for antifibrotic effect on liver fibrosis were tried to identify in advance.
Results: Secreted matrix metalloproteinase (MMP)-14 was found to be a useful predictive factor to reduce liver fibrosis. Moreover, the cutoff index of MMP-14 for 30% reduction of liver fibrosis was 0.918 fg/cell, judging from univariate analysis and receiver operating curve analysis. In addition, MMP-13 activity and thioredoxin contents in IC-2 sheets were also inversely correlated with hepatic hydroxy-proline contents. Finally, IC-2 was also found to promote MMP-14 secretion from BM-MSCs of elderly patients. Surprisingly, the values of secreted MMP-14 from BM-MSCs of elderly patients were much higher than those of young persons.
Conclusion: The results of this study suggest that the IC-2 sheets would be applicable to clinical use in autologous transplantation for patients with cirrhosis regardless of the patient's age.

1. Introduction

Liver fibrosis is caused by an excessive accumulation of the extracellular matrix. Progression of liver fibrosis often leads to liver cirrhosis (LC) [1,2]. Without proper treatment, LC can progress from the early to the decompensated stage, wherein liver function extremely decreases. The medical needs of decompensated LC remain unmet [3–5]. Thus, LC is a major health problem worldwide because the number of mortalities due to LC in 2010 is approximately 50,000 in the USA, 25,000 in Japan, and more than one million worldwide [6]. Most of the causes of LC in the USA include hepatitis C virus, alcoholic liver disease, and non-alcoholic fatty liver disease in adults [7]. Many congenital diseases (e.g., biliary atresia) exist in children [8]. Fontan-associated liver disease (FALD), which develops following the Fontan operation for monoventricular disease, has recently become a problem, and liver fibrosis is a universal feature of FALD [9]. The development of antifibrotic therapy not only cures liver fibrosis but also suppresses the subsequent hepatocellular carcinoma (HCC) incidence because liver fibrosis is strongly associated with HCC incidence [10].

Liver transplantation is the only treatment for decompensated cirrhosis [11]. However, liver transplantation cannot be sufficiently performed due to donor shortage. Moreover, stem cell therapy has recently attracted attention as an alternative treatment to liver transplantation [12,13]. Stem cells include embryonic, induced pluripotent, and somatic stem cells. Mesenchymal stem cells (MSCs), which are one of the somatic stem cells, are derived from mesodermal tissues and can be obtained from bone marrow, adipose tissue, umbilical cord, and so on [14,15]. They have distinctive features such as differentiation plasticity that differentiates ectodermal and endodermal cell lineages [16,17], immunosuppressive ability [18], and secretion of various cytokines [19]. MSCs also have a low risk of tumorigenesis [20]. Due to these advantages, clinical trials using MSCs have been conducted in a wide range of fields, such as autoimmune diseases, cancers, and liver diseases [21–25].

Wnt/β-catenin signaling suppression was previously reported to transdifferentiate bone marrow- and cord blood-derived MSCs into hepatocyte-like cells [26,27]. Based on these findings, IC-2, a newly synthesized derivative of ICG-001, was identified as a potent suppressor of Wnt/β-catenin signaling. Moreover, IC-2 efficiently induced hepatic differentiation of human MSCs [28]. A new therapy, which is a combination of IC-2 treatment and cell sheet technology, was developed to establish a novel therapeutic modality for liver diseases [29,30]. In general, transplantation of cell sheets is superior to cell injection because transplantation of cell sheets avoids the risk of portal vein embolism, has less cell loss, maintains intercellular communications, and delivers uniform and stable cells [31]. The transplantation of IC-2-engineered bone marrow-derived MSC (BM-MSC) sheets (IC-2 sheets) was reported to exert potent regenerative ability and effectively improve acute liver injury in mice [29]. In addition, transplantations of IC-2 sheets dramatically suppressed liver fibrosis in which 47% of hydroxyproline decreased only a week after IC-2 sheet transplantation. Furthermore, matrix metalloproteinase-1 and matrix metalloproteinase-14 (MMP-1 and MMP-14) secreted from IC-2 sheets were found to play a critical role in liver fibrosis reversal [30]. Moving toward the eventual goal of clinical application, IC-2 sheets need further research and development. The efficacy of IC-2 sheets was especially examined from multiple lots of BM-MSCs derived from many donors, particularly from the elderly, and standard items were set for predicting effectiveness.

This study examined the antifibrotic action of IC-2 sheets prepared from commercially purchased multiple lots of BM-MSCs on liver fibrosis. In addition, identifying factors that predict the antifibrotic effect of IC-2 sheets on liver fibrosis was attempted using the supernatants and cell lysates during the manufacturing of IC-2 sheets. Finally, cell viability, Wnt/β-catenin signal intensity, and MMP-14 secretion were examined in response to IC-2 treatment in BM-MSCs obtained from elderly patients who underwent artificial joint replacement to find out whether IC-2 sheets manufactured from elderly donors can be used, since the mean age of patients with cirrhosis at diagnosis is increasingly becoming older annually, which was 68.1 years old in 2014 [32]. Consequently, BM-MSC from the elderly was suggested to at least have the same or better potential as those derived from the youth.

## 2. Materials and methods

2.1. Ethics statements

All methods were carried out in accordance with relevant guidelines and regulations. Animal experiments were conducted in accordance with ARRIVE guidelines [33] and the Tottori University Animal Care and Use Regulations. The study using human bone marrow cells collected from patients who underwent artificial joint replacement at Tottori University Hospital was approved by the Ethics Review Committee of the Faculty of Medicine Tottori University with approval number 1604A006. Informed consent was obtained from each patient.

2.2. Chemical compounds and cells

IC-2, a derivative of ICG-001, was synthesized in-house and dissolved in dimethyl sulfoxide (DMSO) [28]. The DMSO final concentration was 0.1%. Cell sheets were prepared using BM-MSCs that were produced from BM-MNCs (Lonza Inc., Walkersville, MD, USA) for *in vivo* study of transplantation experiments. BM-MSCs from 15 donors were passaged 2 to 5 times, and 29 lots of BM-MSCs were finally obtained. The cells were then cryopreserved until use for cell sheet preparation. Bone marrow cells collected from 50- to 79-year-old patients who underwent artificial joint replacement at Tottori University Hospital were used (Table S3) for *in vitro* study. Moreover, the study was approved by the Ethics Review Committee of the Faculty of Medicine Tottori University with approval number 1604A006. Informed consent was obtained from each patient. Culture dish-adherent BM-MSCs were prepared after density centrifugation of bone marrow in Ficoll–Paque PLUS (GE Healthcare UK Ltd., Little Chalfont, UK), and obtained MSCs were passaged a few times and cryopreserved until use.

2.3. Fluorescence-activated cell sorter analysis

The characteristic surface markers of MSCs [34] were examined by FACS analysis. Cells were washed with phosphate-buffered saline containing 0.5% bovine serum albumin and 1 mM EDTA. The cells were then incubated with the antibodies to CD34-APC, CD45-APC, HLA-DR-FITC (1:40; Thermo Fisher Scientific Inc., Waltham, MA, USA), CD90-APC (1:100; BD Biosciences, San Jose, CA, USA), and CD105-FITC (1:20; Bio-Rad Laboratories, Inc., Irvine, CA, USA) for 30 min at 4 °C. IgG1-FITC (1:40; Miltenyi Biotec GmbH, Bergisch Gladbach, Germany), IgG1-APC, and IgG2a-FITC (1:40; Thermo Fisher Scientific, Inc.) were used as isotype-matched negative controls. Propidium iodide was used to remove nonviable cells. Moreover, cell surface marker expression was analyzed by Gallios (Beckman Coulter, Brea, CA, USA). Furthermore, data were analyzed using FlowJo software (Tree Star, Inc., Ashland, OR, USA).

a

b

c
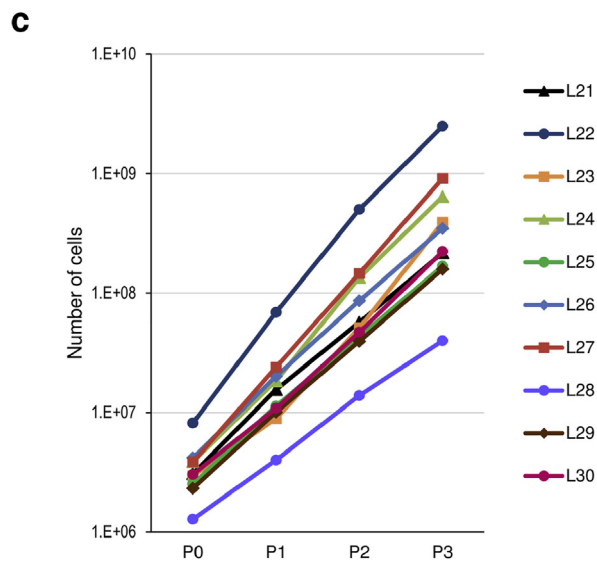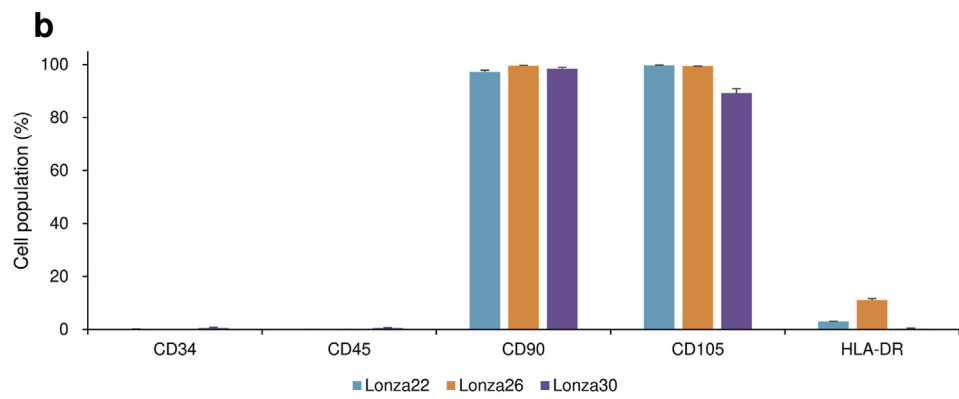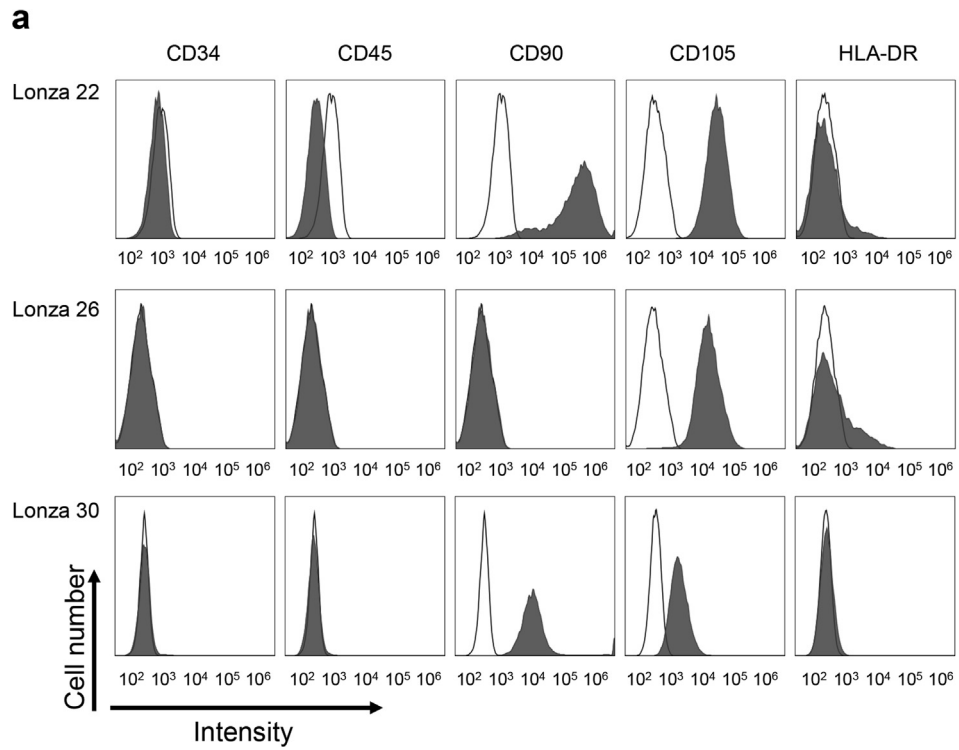
2.4. Preparation of cell sheets and parameters

IC-2 sheets were manufactured as follows. Cells that had been frozen were passaged three to five times and then plated on ϕ 60-mm temperature-responsive culture dishes (Cell Seed Inc., Tokyo, Japan) at a seeding density of 5.4×10^4 cells/cm^2. Furthermore, cells were treated with 30 μM IC-2 on a ϕ 60-mm temperature-responsive culture dish the next day for a week. The medium was changed 4 days after the start of incubation. Cell sheets, called IC-2 sheets, were harvested by incubating at 20 °C and storing at 20 °C until transplantation. The parameters of each cell sheet included MMP-1 content, MMP-14 content, MMP-2 activity, MMP-13 activity, thioredoxin content, amphiregulin content, and C3 content in the supernatants collected from cell culture from 4 to 7 days. Active MMP-1 activity, total MMP-1 activity, active MMP-14 activity, total MMP-14 activity, MMP-2 activity, MMP-13 activity, and thioredoxin content were measured with the other cell sheets prepared in the same manner for transplantation.

2.5. Animal experiments

All animal experiments were conducted following the ethical approval of the Tottori University Subcommittee on Laboratory Animal Care (approved number: 16-Y-28). All mice were housed under pathogen-free conditions in a temperature-controlled, illuminated (12 h daily) room with ad libitum access to water and chow. To induce chronic liver injury, carbon tetrachloride (CCl₄; Wako Pure Chemical Industries Ltd., Osaka, Japan) dissolved in olive oil (Wako Pure Chemical Industries Ltd.) was orally administered twice per week to 7-week-old BALB/c-nu/nu male mice (CLEA Japan, Inc., Tokyo, Japan) at a dose of 0.6 and 1.2 mL/kg for 4 and another 6 weeks, respectively.

2.6. Transplantation of cell sheets

Transplantation of cell sheets was performed 2 days after the last administration of CCl₄ in CCl₄-treated BALB/c-nu/nu mice. Three-layered cell sheets were transplanted at one site on the left lateral lobe. Control mice were operated on using sham laparotomy. CCl₄ administration was continued for another week after transplantation. Mice were sacrificed by exsanguination with sodium pentobarbital 2 days after the final administration of CCl₄, and blood samples were collected from the inferior vena cava, followed by hepatectomy. Part of the liver was fixed with 4% paraformaldehyde and embedded in paraffin for histological analysis. The remaining liver tissue was snap-frozen in liquid nitrogen.

2.7. Biochemical tests

Blood samples were maintained overnight on ice, and serum was isolated by centrifugation at 2000×g for 20 min. Serum aminotransferase and total bilirubin levels were measured as previously reported [29,30]. Serum total protein and albumin levels were measured using DRI-CHEM NX700V (FUJIFILM, Tokyo, Japan).

2.8. Histological analyses

Paraffin embedded livers were sectioned to 3-μm-thick sections for Sirius Red staining and 2-μm-thick sections for Azan staining. Sirius Red staining was performed with the picrosirius red staining kit (Polysciences, Inc., Warrington, PA) according to the manufacturer's protocol. Azan staining was performed by standard methods. The ratio of fibrosis area was measured using a BZ-X Analyzer (Keyence Japan, Osaka, Japan) and we measured 4 to 5 fields per mouse.

2.9. Hydroxyproline contents

Hydroxyproline contents were measured as previously described [35]. A liver tissue piece (100 mg wet weight) was homogenized in 1 mL of distilled water, and an equal volume of 12 N concentrated hydrochloric acid was added to 100 μL of this slurry. Furthermore, the mixture underwent hydrolysis in a block incubator (IKA, Staufen, Germany) at 120 °C. The mixture was cooled at room temperature after hydrolysis treatment and centrifuged at room temperature at 3000 rpm for 5 min after pipetting. After centrifugation, 10 μL of the supernatant was transferred to a 1.5-mL tube, and hydrochloric acid was removed with an evaporator (Sakuma Seisakusho, Tokyo, Japan). Subsequently, hydroxyproline was measured using a Hydroxyproline Quantification Kit (Bio-Vision, CA, USA), according to the manufacturer's instructions. The amount of protein in the tissue homogenate was measured by the Bradford method using a protein assay concentrated dye reagent (Bio-Rad, Hercules, CA, USA). The amount of hydroxyproline per unit protein amount was determined to evaluate the fibrosis level.

2.10. Western blot analysis

Alpha-smooth muscle actin (α-SMA) expression was examined by Western blot analysis because it was a major indicator of hepatic stellate cells (HSCs) activation which induced liver fibrosis [1,2,36]. Ten milligrams of proteins were subjected to Western blot analysis as previously described [29,30]. Mouse monoclonal antibodies including anti-αSMA (DakoCytomation, Agilent Technologies, Inc., Santa Clara, CA, USA) and anti-GAPDH antibody (MilliporeSigma, Burlington, MA, USA) were used. Chemiluminescent images were acquired by ImageQuant LAS-4000 (GE Healthcare UK Ltd.) with ECL Prime Western Blotting Detection Reagent (GE Healthcare UK Ltd.).

2.11. WST assay

At 24 h after seeding of BM-MSCs at a density of 5.4×10^4 cells/cm^2, 20–50 μM of IC-2 were added. WST assay was performed with Cell Counting Kit-8 (Dojindo Molecular Technologies, Inc., Kumamoto, Japan) using Sunrise Rainbow RC plate reader (Tecan Group Ltd., Mannedorf, Switzerland) 7 days after addition.

2.12. Reporter assay

At 24 h after seeding of BM-MSCs at a density of 5.4×10^4 cells/cm^2, 20–50 μM IC-2 was added. The TCF/LEF reporter lentivirus

Fig. 1. Characterization of cell surface markers of MSCs by flow cytometry. (a) Representative histogram of the FACS of cell surface marker expression on BM-MSCs used in the present study. BM-MSCs from Lonza 22, Lonza 26, and Lonza 30 at passage 3 were labeled with FITC-coupled antibodies against CD34, CD45, CD90, CD105, and HLA-DR. *Shaded areas* indicated staining with antibodies against the indicat antigens, and *solid lines* indicate background fluorescence stained with isotype control. (b) *Grouped bar chart* showing quantitation of cell surface markers on each lot of three donors-derived BM-MSCs. The data are presented as mean ± SD from three independent FACS analyses. (c) The growth curve of the ten lots of BM-MSCs from L21 (Lonza 21) to L30 (Lonza 30). Cell culture was started at a cell density of 5.0×10^3 to 1.0×10^4 cells/cm^2 (P0) and passaged every 3–4 days to P1, P2, and P3.

(SABiosciences, Qiagen N.V., Frederick, MD, USA) and control renilla lentivirus (SABiosciences, Qiagen N.V.) were transduced, and reporter assay was performed using luciferase assay system (Promega Corp.) as previously described 4 days after addition [28].

2.13. RNA extraction and quantitative RT-PCR analysis

Total RNA was extracted using TRIzol reagent (Invitrogen, Life Technologies Corp., Carlsbad, CA, USA). Reverse transcription was performed using SuperScript II First-Strand Synthesis System for reverse transcription-polymerase chain reaction (RT-PCR; Invitrogen) and oligo(dt)$_{18}$ primers, according to the manufacturer's instructions. Real-time PCR analysis was performed using Light-Cycler Fast DNA Master SYBR Green I (Roche Diagnostics GmbH, Mannheim, Germany). Primers for qRT-PCR analysis were as follows: MMP14-forward, 5′-CCTACCGACAAGATTGATGCTG-3′; MMP14-reverse, 5′-AAACGGTAGTACTTGTTTCCACG-3′; GAPDH-forward, 5′-AGCCACATCGCTCAGACAC-3′; and GAPDH-reverse, 5′-GCCCAATACGACCAAATCC-3′. Furthermore, PCR was performed for each assay using a 7900 HT Fast Real-Time PCR System (Applied Biosystems, Life Technologies Corp., Carlsbad, CA, USA).

2.14. Enzyme-linked immunosorbent assay

The culture supernatants of each cell culture were collected and stored at −80 °C until analysis. According to the manufacturer's instructions, MMP-1, MMP-14, complement component C3, amphiregulin, and thioredoxin contents in the culture supernatants were quantified using Human MMP1 Enzyme-Linked Immunosorbent Assay (ELISA) Kit (Abcam Ltd., Cambridge, UK), Human MMP14 ELISA Kit (Abcam Ltd., Cambridge, UK), Human Complement C3 ELISA Kit (Abcam Ltd., Cambridge, UK), Quantikine® Human Amphiregulin ELISA Kit (R&D Systems, Inc., Minneapolis, MN, USA), and Human TXN/Thioredoxin/TRX ELISA Kit (LifeSpan BioSciences, Inc., Seattle, WA, USA), respectively.

2.15. Matrix metalloproteinase activity assay

Culture supernatants were collected 7 days after the IC-2 treatment, and cells were homogenized in the lysis buffer provided with the following assay kits: SensoLyte® 520 MMP-1 Assay Kit *Fluorimetric*, SensoLyte® 520 MMP-14 Assay Kit, SensoLyte® Plus 520 MMP-2 Assay Kit, and SensoLyte® Plus 520 MMP-13 Assay Kit (AnaSpec, Inc., CA, USA). Samples were stored at −80 °C until analysis, and each MMP activity was measured according to the manufacturer's instructions.

2.16. Statistical analyses

All the values were expressed as means ± SD. Student's *t*-test was performed to compare the means of response variable between the two groups using Microsoft Excel. Moreover, Steel tests (http://www.gen-info.osaka-u.ac.jp/MEPHAS/s-d.html) were conducted to compare the difference among the three groups. *P* values <0.05 were considered to be statistically significant. Dunnett's test, univariate analysis, and multivariate statistical analysis were performed using SPSS Statistics (IBM SPSS Statistics; IBM Corp., Armonk, NY, USA).

3. Results

3.1. Characteristics of MSCs prepared from commercial bone marrow-derived mononuclear cells (BM-MNCs)

Previous reports revealed that transplantation of IC-2 sheets consisted of hepatic differentiated BM-MSCs ameliorated CCl$_4$-

induced acute and chronic liver injury. These observations were obtained from the data using an immortalized BM-MSC cell line or primary MSCs generated from a single donor-derived BM-MSCs [29,30]. This study prepared 15 donors-derived BM-MSCs and the presence of mesenchymal lineage-associated cell surface markers was confirmed with fluorescence-activated cell sorting (FACS) analysis. The cells from Lonza 22, Lonza 26, and Lonza 30 were negative for CD34 and CD45 (Fig. 1a) but positive for CD90 and CD105. Little expression of HLA-DR was observed in the cells of three donors. The growth curve of the cells demonstrated that active cell proliferation was observed in all ten cells at passage 3 (Fig. 1c). These data suggest that the cells used in the experiments share the common features of BM-MSCs, as described in the methods section.

3.2. IC-2 sheets ameliorated liver fibrosis in mice

This study generated 29 lots of BM-MSCs from 15 donors by altering the passage numbers of cells from passages 2 to 5 to evaluate whether IC-2 sheets generated from BM-MSCs from different persons have antifibrotic action. IC-2 sheets fabricated from each lot of BM-MSCs were transplanted onto the liver surface of each mouse. Consequently, mice received three-layer IC-2 sheets at one site (IC-2 group) after 10 weeks of CCl$_4$ intoxication. Sham-operated mice (sham group) served as the control. Liver fibrosis, quantified by Azan and Sirius red staining, was markedly reduced in the IC-2 group than in the sham group, accompanied by improvement of pseudolobule-like structure observed in the sham group, regardless of the difference of cell sheets (Fig. 2a–d). Three outliers were excluded due to the interquartile range when 29 samples of hydroxyproline contents were statistically examined. Hepatic hydroxyproline contents were compared among 22, 26, and 3 samples for the sham, IC-2, and CCl$_4$(−) groups, respectively. Furthermore, hepatic hydroxyproline content was significantly reduced in the IC-2 group than in the sham group (Fig. 2e). Moreover, hepatic stellate cells (HSCs) activation was examined by alpha-smooth muscle actin (α-SMA) expression, an indicator of promoting fibrogenesis. The α-SMA expression was remarkably reduced in the IC-2 group, suggesting that IC-2 sheets suppressed fibrogenesis in mice livers (Fig. 2f). In addition, serum alanine transaminase (ALT) and total bilirubin were significantly decreased in the IC-2 group, whereas serum aspartate transaminase (AST) was not changed (Fig. 2g). Both the total protein and albumin levels were not also affected by sheets transplantation (Fig. S1). Thus, IC-2 sheets also improved liver damage besides reducing liver fibrosis. These data suggest that IC-2 sheets generated from miscellaneous patients will be expected to exert a potent effect when applied in clinical settings.

3.3. Secreted MMP-14 was a predictor for therapeutic efficacy for liver fibrosis

Identifying parameters that predict the antifibrotic effect of IC-2 sheets was next attempted because IC-2 sheets generated from BM-MSCs originating from different persons demonstrated to have antifibrotic action. The parameters involved in fibrosis and liver regenerations measured in the supernatants of cultured cells and cell lysates were included in the analysis. Five samples were excluded from the statistical analysis because cell count was not performed in five samples (Tables S1 and S2). First, a univariate analysis was done between hepatic hydroxyproline contents and cell sheets-secreted factors (Table 1 and Table S1). Of the seven parameters, MMP-14 was inversely correlated with hepatic hydroxyproline contents (Fig. 3; *P* = 0.012). The MMP-14 value was measured in the conditioned media cultured from days 4–7 after
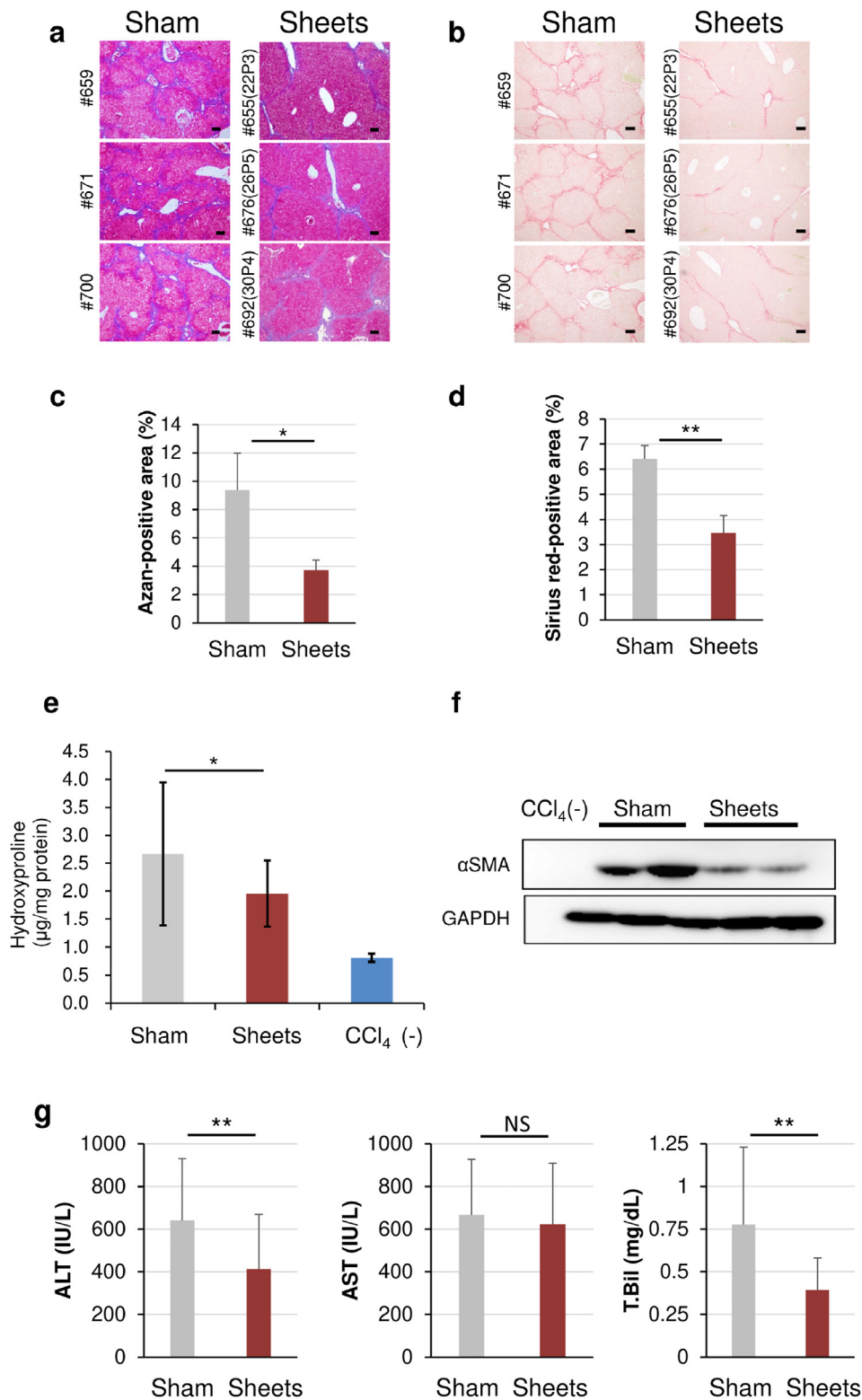
Fig. 2. Regression of liver fibrosis by IC-2 sheets. (a) Micrographs of liver sections subjected to Azan staining. The individual number of the mouse (lot number of the cell sheet) is described on the left side of each micrograph (scale bar = 100 μm). (b) Sirius Red staining (scale bar = 100 μm). (c) The proportions of Azan-stained fibrotic areas of two groups (4—5 fields per each mouse in 3 mice were measured). (d) The proportions of Sirius Red-stained fibrotic areas of two groups (4—5 fields per mouse in 3 mice were measured). (e) Hydroxyproline contents in the liver. The number of mice examined in the sham, sheets, and CCl4(−) groups were 22, 26, and 3, respectively. *P < 0.05 examined by Steel test. (f) α-SMA expression in recipient liver tissues was measured by western blotting. Sham and sheets represent the sham and IC-2 sheets groups, respectively. (g) Serum aspartic aminotransferase, alanine aminotransferase, and total bilirubin were shown. The number of mice examined in the sham, sheets, and CCl4(−) groups was 22, 26, and 3, respectively, except 24 of the total bilirubin in the sheets group. The results are expressed as mean ± S.D. **P < 0.01 examined by Student's t-test.

Table 1
Univariate analysis between hepatic hydroxyproline contents and cell sheets-secreted factors.

Parameter	Univariate analysis	
	β-value	P-value
MMP-1 (fg/cell)	−0.214	0.351
MMP-2 activity (fg/cell)	−0.338	0.135
MMP-13 activity (fg/cell)	−0.331	0.143
MMP-14 (fg/cell)	−0.578	0.012[*]
Thioredoxin (fg/cell)	−0.006	0.98
Amphiregulin (fg/cell)	−0.215	0.349
C3 (pg/cell)	−0.226	0.325

MMP, matrix metalloproteinase; [*]P < 0.05.

Table 2
Univariate analysis between hepatic hydroxyproline contents and factors in lysates of cell sheets.

Parameter	Univariate analysis	
	β- value	P-value
MMP-1 activity (RFU/cell)	−0.238	0.299
MMP-2 activity (fg/cell)	−0.266	0.245
MMP-13 activity (fg/cell)	−0.482	0.043[*]
MMP-14 activity (RFU/cell)	−0.380	0.089
Thioredoxin (fg/cell)	−0.516	0.017[*]

MMP, matrix metalloproteinase; RFU, relative fluorescence units; [*]P < 0.05.

the addition of IC-2. Consequently, hepatic hydroxyproline content was measured at 7 days after transplantation. These data suggest that secreted MMP-14 during manufacturing cell sheets is an advanced predictor for the antifibrotic effect of IC-2 sheets. Second, a univariate analysis was performed among hepatic hydroxyproline contents and factors in lysates of cell sheets (Table 2 and Table S2). The cell lysates were examined in the other cell sheets prepared in the same manner for transplantation. Of the five parameters, MMP-13 activity and thioredoxin content were inversely correlated with hepatic hydroxyproline contents (Fig. S2; $P = 0.043$ and $P = 0.017$, respectively). Consistent with the activation of MMP-13, a well-known role of MMP-14, intracellular MMP-13 activity was observed to be significantly correlated with extracellular MMP-14
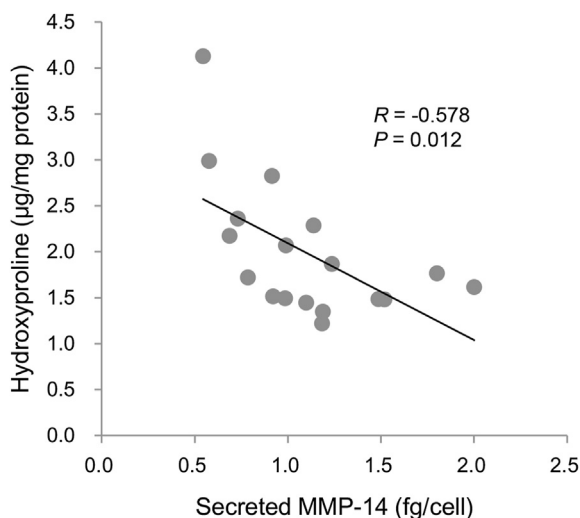

Fig. 3. Secreted MMP-14 from IC-2 sheets is inversely correlated with hepatic hydroxyproline contents. Secreted MMP-14 contents in the conditioned media during manufacturing IC-2 sheets from days 4—7 were measured and expressed as per cell. Hepatic hydroxyproline contents at 7 days after transplantation were analyzed.

contents ($P = 0.02$, data not shown). The analysis of the receiver operating curve indicated that the area under the curve for secreted MMP-14 was 0.917, suggesting that MMP-14 can predict a 30% decrease in hydroxyproline contents ($P = 0.005$; Fig. S3). The cutoff index of MMP-14 contents in the supernatants of culture media for prediction of 30% suppression of liver fibrosis was 0.918 fg/cell).

3.4. BM-MSCs derived from the elderly have similar characteristics to those derived from young people

Growth, Wnt/β-catenin signal, and MMP-14 production in response to IC-2 in BM-MSCs from the elderly were examined because cirrhosis is known to develop in elderly as mentioned above. BM-MSCs were collected from six patients (50 − 79 years old) who underwent artificial joint replacement. All patients had coxarthrosis (Table S3). The cell viability of BM-MSCs was decreased with IC-2 concentration, which was about 70 − 80% in patients 1, 2, and 3 at 30 μM IC-2 (Fig. 4a). The Wnt/β-catenin signal intensity was suppressed at 40%−50% at 30 μM IC-2, which is similar to the data of BM-MSCs from the youth reported in reference 28 (Fig. 4b). The supernatants of day 4 to day 7 culture and day 7 to day 9 culture after IC-2 treatments were collected from BM-MSCs at 7 and 9 days, respectively, and MMP-14 contents were then measured in patients 1 and 6. The MMP-14 values corrected by cell number were markedly increased by the IC-2 treatment compared with the control (Fig. 5a). Surprisingly, the average values of secreted MMP-14 ranged between 3 and 6 fg/cell in 2−3 days, which were higher than the present study where BM-MSCs from young persons were used. Intracellular MMP-14 contents were also higher compared with the control in the IC-2-treated cells from patients 4 and 5 (Fig. 5b). The MMP-14 mRNA expression was also upregulated compared with the control in the IC-2-treated cells, except for patient 4 who tended upregulation without statistical significance (Fig. 5c). Taken together, these data suggest that BM-MSCs obtained from the elderly can be used as a cell source for IC-2 sheets.

4. Discussion

This study demonstrated the antifibrotic action of IC-2 sheets generated from commercially purchased different lots of BM-MSCs. These data suggest that autologous transplantation of IC-2 sheets will be effective for patients with LC in the future. In addition, the practical application of IC-2 sheets will be realized in elderly and young patients.

In the present study, ALT was decreased, but AST was not decreased by the IC-sheets. The question why only ALT was decreased but AST was not decreased was raised (Fig. 2g). The differences of ALT and AST may be affected by both timing of peak and half-life of transaminases after liver injury. The half-life of ALT is about 36 h, and that of AST is about 18 h [37]. In addition, transaminases peak at 6 h after CCl_4 administration in cases of male rats [38]. Therefore, changes of ALT may be prolonged longer than those of AST. In the present study, mice were sacrificed at 48 h after the final CCl_4 treatment. Measurement of transaminases at 48 h after liver injury may cause only difference in ALT, but not in AST.

Of the seven parameters in the supernatant of the culture medium during manufacturing IC-2 sheets, MMP-14 is inversely correlated with liver fibrosis, suggesting that MMP-14 is an advanced predictor of liver fibrosis regression. In addition, the cutoff index for the prediction of the 30% suppression of liver fibrosis was 0.918 fg/cell. These data were supported by a previous report stating that MMP-14 derived from IC-2 sheets is responsible for the antifibrotic effects on liver fibrosis [30]. In general, hepatocytes do not express MMPs, however, some MMPs are produced
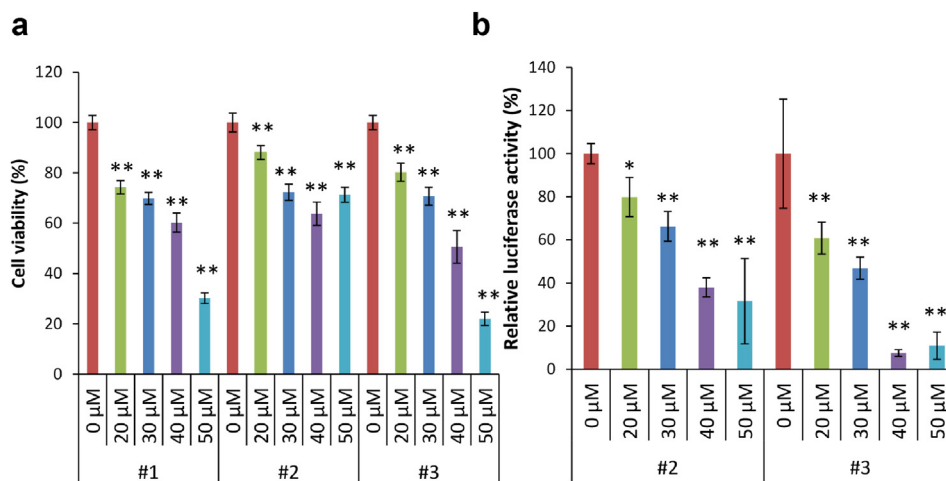
Fig. 4. Cell viability and Wnt/β-catenin signal intensity in response to IC-2. (a) Cell viability by WST assay in various concentrations of IC-2 ($n = 3$). Mean ± SD, $^*P < 0.05$, and $^{**}P < 0.01$ compared with 0.1% DMSO, examined by Dunnett's test. (b) Wnt/β-catenin signal intensity in response to various concentrations of IC-2 by reporter assay ($n = 3$). Mean ± SD, $^*P < 0.05$, and $^{**}P < 0.01$ compared with 0.1% DMSO, examined by Dunnett's test. Relative luciferase activity was expressed as corrected firefly luciferase activity with the internal control renilla luciferase activity calculated against 0.1% DMSO.
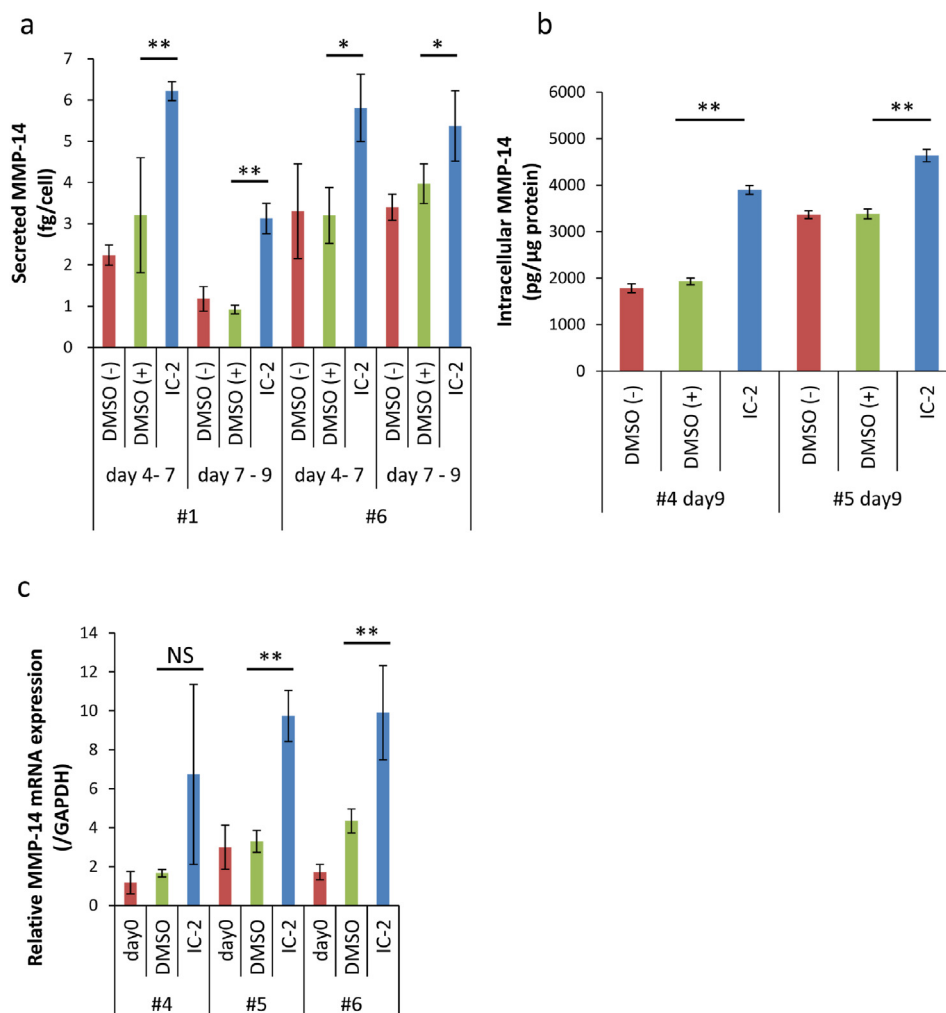

Fig. 5. MMP-14 in response IC-2 in BM-MSCs from the elderly. (a) Secreted MMP-14 in the culture supernatant of BM-MSCs from the elderly in IC-2-contained medium ($n = 3$). The supernatants of 3 days culture (day 4–7) and 2 days culture (day 7–9) culture were collected from BM-MSCs at 7 and 9 days after IC-2 treatments, respectively. Mean ± SD, $^*P < 0.05$, and $^{**}P < 0.01$ compared with DMSO (+) examined by Dunnett's test. (b) Intracellular MMP-14 contents of BM-MSCs from the elderly with IC-2 treatment ($n = 3$). Cells were harvested and examined at end point of culture (day 9). Mean ± SD, $^*P < 0.05$, and $^{**}P < 0.01$ compared with DMSO (+) examined by Dunnett's test. (c) MMP-14 mRNA expression of BM-MSCs from the elderly after IC-2 treatment ($n = 3$). Mean ± SD, $^*P < 0.05$, and $^{**}P < 0.01$ compared to DMSO treatment, examined by Dunnett's test.

by hepatocytes under certain conditions [39]. Therefore, it is not surprising that some MMPs are elevated in IC-2-induced hepatic cells. Hexachlorophene was known to be another Wnt/β-catenin signal inhibitor and an inducer of hepatic differentiation in our previous reports [28,29,40]. 0.8 μM hexachlorophene treatment for 7 days did not induce MMP-1, MMP-2, or MMP-14 expression (Fig. S4), although 0.8 μM hexachlorophene suppressed Wnt/β-catenin signal more potently than 20 μM IC-2 (data not shown). These data suggest that induction of MMP-14 by IC-2 treatment was not due to the results of Wnt/β-catenin signal inhibition or hepatic differentiation of MSCs. Taken together, induction of MMPs is a unique action of IC-2 in MSCs. MMP-14 can break down type I collagen, a major component of the extracellular matrix of the fibrotic liver [41]. Taken together, MMP-14 plays a crucial role in the fibrinolysis of the IC-2 sheets. Furthermore, MMP-13 activity in the cell lysate was found to be inversely correlated with hepatic hydroxyproline contents. Increases in MMP-13 activity may be due to the MMP-14 upregulation because MMP-13 has been reported to be activated by MMP-14 [42,43]. Moreover, intracellular thioredoxin contents were also inversely correlated with hepatic hydroxyproline. Thioredoxin is essential for reducing oxidative stress and suppression of activated HSCs [40,44,45]. In a previous report, thioredoxin secretion was enhanced in mesenchymal stem cell-derived cell sheets treated with IC-2 [30]. Taken together, hepatic cells differentiated by Wnt/β-catenin signal inhibitors were converted to produce thioredoxin.

Moreover, this study found that MMP-14 was induced by IC-2 in BM-MSCs from elderly persons. Surprisingly, the average values of secreted MMP-14 ranged between 3 and 6 fg/cell, which was higher compared with the cells from young persons. These data suggest that IC-2 sheets generated from elderly persons are expected to demonstrate highly therapeutic effects. It is generally supposed that the quality of MSCs, assessed by proliferative and differentiation abilities, declines with age [46,47]. However, IC-2 can induce more MMP-14 production in BM-MSCs from elderly persons compared to young persons in the present study. Although we did not measure MMP-14 levels before treatment with IC-2 in MSCs of young persons, MMP-14 production after treatment with IC-2 was 1.1 ± 0.4 fg/cell (Table S1), which was lower than that of the elderly patients (Fig. 5a). The hypothesis that characteristics of MSCs are different between younger and older MSCs was raised. This hypothesis is supported by the paper that MMP-14 expression is elevated with aging in the extracellular matrix (ECM) fraction of left ventricle [48]. Furthermore, higher MMP-14 levels in ECM fraction of left ventricle have been reported in patients with chronic hypertension [49]. These two reports suggest that characteristics of MSCs change with aging in response to remodeling of ECM. In fact, MMP-14 in #6 patient with hypertension was higher than those without hypertension in our patients. Since the exact mechanism of promoting MMP-14 production by treatment with IC-2 is unclear, this issue has to be clarified in the future. Especially, whether MMP-14 was also induced by treatment with IC-2 in liver progenitor cells such as ES cells-derived, iPS cells-derived, and adipose tissue-derived stem cells-derived cells is a matter of investigation in the near future.

Identifying markers to predict effects in advance is important in clinical practice, and these markers are desirably based on the mechanisms of action. In a study of autologous transplantation of skeletal muscle cell sheets for severe heart failure, the authors suggest that therapeutic effects are based on the factors that induce angiogenesis and antioxidant activity, such as stromal-derived factor 1, hepatocyte growth factor, and vascular endothelial growth factor [50–52]. Moreover, this report is believed to be the first to identify predictable markers involved in the effectiveness of therapy based on mechanisms of action in liver diseases. Taken

together, the cutoff index setting of MMP-14 will greatly contribute to the improvement of IC-2 sheet therapy for LC.

5. Conclusions

This study found that IC-2-engineered mesenchymal stem cell sheets generated from different persons reduced liver fibrosis and secreted MMP-14 in the supernatant is a predictor for the therapeutic effect on liver fibrosis. In addition, BM-MSCs from elderly persons are expected to exert potent antifibrotic effects. Thus, the IC-2 sheets would be applicable for clinical use in autologous transplantation for patients with cirrhosis regardless of the patient's age.

Declaration of competing interest

G.S. holds more than 5% of the total shares of KanonCure Inc. and receives compensation as a member of KanonCure Inc. The other authors have no competing interests to declare.

Tottori university and KanonCure Inc. have the patents for IC-2 sheets (patent registration numbers, US 9,555,061, DE602012040872.3, ES2698365, FR2698365, GB269835, and IT502018000006592), and patent applications (patent application numbers TW107129167, US16/641,874, CN201880054224.7, EP18851336.0, PCT/JP2019/021603, US16/972,285, and EP198156721).

Appendix A. Supplementary data

Supplementary data to this article can be found online at https://doi.org/10.1016/j.reth.2021.08.004.

References

[1] Tsuchida T, Friedman SL. Mechanisms of hepatic stellate cell activation. Nat Rev Gastroenterol Hepatol 2017;14:397–411.
[2] Ge PS, Runyon BA. Treatment of patients with cirrhosis. N Engl J Med 2016;375:767–77.
[3] Su TH, Kao JH. Unmet needs in clinical and basic hepatitis B virus research. J Infect Dis 2017;216:S750–6.
[4] Trautwein C, Friedman SL, Schuppan D, Pinzani M. Hepatic fibrosis: concept to treatment. J Hepatol 2015;62:S15–24.
[5] Torok NJ, Dranoff JA, Schuppan D, Friedman SL. Strategies and endpoints of antifibrotic drug trials: summary and recommendations from the AASLD Emerging Trends Conference, Chicago, June 2014. Hepatology 2015;62:627–34.
[6] Mokdad AA, Lopez AD, Shahaz S, Lozano R, Mokdad AH, Stanaway J, et al. Liver cirrhosis mortality in 187 countries between 1980 and 2010: a systematic analysis. BMC Med 2014;12:145.
[7] Beste LA, Leipertz SL, Green PK, Dominitz JA, Ross D, Ioannou GN. Trends in burden of cirrhosis and hepatocellular carcinoma by underlying liver disease in US veterans, 2001-2013. Gastroenterology 2015;149:1471–82.
[8] Olave MC, Gurung A, Mistry PK, Kakar S, Yeh M, Xu M, et al. Etiology of cirrhosis in the young. Hum Pathol 2020;96:96–103.
[9] Gordon-Walker TT, Bove K, Veldtman G. Fontan-associated liver disease: a review. J Cardiol 2019;74:223–32.
[10] Zhang DY, Friedman SL. Fibrosis-dependent mechanisms of hepatocarcinogenesis. Hepatology 2012;56:769–75.
[11] Choudhary NS, Saraf N, Saigal S, Soin AS. Liver transplantation for acute on chronic liver failure. J Clin Exp Hepatol 2017;7:247–52.
[12] Stutchfield BM, Forbes SJ, Wigmore SJ. Prospects for stem cell transplantation in the treatment of hepatic disease. Liver Transplant 2010;16:827–36.

[13] Kuo TK, Hung SP, Chuang CH, Chen CT, Shih YR, Fang SC, et al. Stem cell therapy for liver disease: parameters governing the success of using bone marrow mesenchymal stem cells. Gastroenterology 2008;134:2111–21.

[14] Uder C, Brückner S, Winkler S, Tautenhahn HM, Christ B. Mammalian MSC from selected species: features and application. Cyometry A 2018;93A:32–49.

[15] Erices A, Conget P, Minguell JJ. Mesenchymal progenitor cells in human umbilical cord blood. Br J Haematol 2000;109:235–42.

[16] Pittenger MF, Mackay AM, Beck SC, Jaiswal RK, Douglas R, Mosca JD, et al. Multilineage potential of adult human mesenchymal stem cells. Science 1999;284:143–7.

[17] Ding DC, Shyu WC, Chiang MF, Lin SZ, Chang YC, Wang HJ, et al. Enhancement of neuroplasticity through upregulation of beta1-integrin in human umbilical cord-derived stromal cell implanted stroke model. Neurobiol Dis 2007;27:339–53.

[18] Cao W, Cao K, Cao J, Wang Y, Shi Y. Mesenchymal stem cells and adaptive immune responses. Immunol Lett 2015;168:147–53.

[19] Park CW, Kim KS, Bae S, Son HK, Myung PK, Hong HJ, et al. Cytokine secretion profiling of human mesenchymal stem cells by antibody array. Int J Stem Cells 2009;2:59–68.

[20] Bernardo ME, Zaffaroni N, Novara F, Cometa AM, Avanzini MA, Moretta A, et al. Human bone marrow derived mesenchymal stem cells do not undergo transformation after long-term in vitro culture and do not exhibit telomere maintenance mechanisms. Cancer Res 2007;67:9142–9.

[21] Wakitani S, Okabe T, Horibe S, Mitsuoka T, Saito M, Koyama T, et al. Safety of autologous bone marrow-derived mesenchymal stem cell transplantation for cartilage repair in 41 patients with 45 joints followed for up to 11 years and 5 months. J Tissue Eng Regen Med 2011;5:146–50.

[22] Dotoli GM, De Santis GC, Orellana MD, de Lima Prata K, Caruso SR, Fernandes TR, et al. Mesenchymal stromal cell infusion to treat steroid-refractory acute GvHD III/IV after hematopoietic stem cell transplantation. Bone Marrow Transplant 2017;52:859–62.

[23] Bartolucci J, Verdugo FJ, González PL, Larrea RE, Abarzua E, Goset C, et al. Safety and efficacy of the intravenous infusion of umbilical cord mesenchymal stem cells in patients with heart failure: a phase 1/2 randomized controlled trial (RIMECARD trial [randomized clinical trial of intravenous infusion umbilical cord mesenchymal stem cells on cardiopathy]). Circ Res 2017;121:1192–204.

[24] Suk KT, Yoon JH, Kim MY, Kim CW, Kim JK, Park H, et al. Transplantation with autologous bone marrow-derived mesenchymal stem cells for alcoholic cirrhosis: phase 2 trial. Hepatology 2016;64:2185–97.

[25] Wang S, Qu X, Zhao RC. Clinical applications of mesenchymal stem cells. J Hematol Oncol 2012;5:19.

[26] Shimomura T, Yoshida Y, Sakabe T, Ishii K, Gonda K, Murai R, et al. Hepatic differentiation of human bone marrow-derived UE7T-13 cells: effects of cytokines and CCN family gene expression. Hepatol Res 2007;37:1068–79.

[27] Yoshida Y, Shimomura T, Sakabe T, Ishii K, Gonda K, Matsuoka S, et al. A role of Wnt/β-catenin signals in hepatic fate specification of human umbilical cord blood-derived mesenchymal stem cells. Am J Physiol Gastrointest Liver Physiol 2007;293:G1089–98.

[28] Itaba N, Sakabe T, Kanki K, Azumi J, Shimizu H, Kono Y, et al. Identification of the small molecule compound which induces hepatic differentiation of human mesenchymal stem cells. Regen Ther 2015;2:32–41.

[29] Itaba N, Noda I, Oka H, Kono Y, Okinaka K, Yokobata T, et al. Hepatic cell sheets engineered from human mesenchymal stem cells with a single small molecule compound IC-2 ameliorate acute liver injury in mice. Regen Ther 2018;9:45–57.

[30] Itaba N, Kono Y, Watanabe K, Yokobata T, Oka H, Osaki M, et al. Reversal of established liver fibrosis by IC-2-engineered mesenchymal stem cell sheets. Sci Rep 2019;9:6841.

[31] Ohashi K, Yokoyama T, Yamato M, Kuge H, Kanehiro H, Tsutsumi M, et al. Engineering functional two- and three-dimensional liver systems in vivo using hepatic tissue sheets. Nat Med 2007;13:880–5.

[32] Enomoto H, Ueno Y, Hoasa Y, Nishikawa H, Hige S, Takikawa Y, et al. Japan Etiology of Liver Cirrhosis Study Group in the 54th annual meeting of JSH.

[33] du Sert NP, Hurst V, Ahluwalia A, Alam S, Avey MT, Baker M, et al. The ARRIVE guidelines 2.0: updated guidelines for reporting animal research. PLoS Biol 2020;18:e3000410. https://doi.org/10.1371/journal.pbio.3000410.

[34] Pendleton C, Li Q, Chesler DA, Yuan K, Guerrero-Cazares H, Quinones-Hinojosa A. Mesenchymal stem cells derived from adipose tissue vs bone marrow: in vitro comparison of their tropism towards gliomas. PLos One 2013;8:e58198.

[35] Cissell DD, Link JM, Hu JC, Athanasiou KA. A modified hydroxyproline assay based on hydrochloric acid in Ehrlich's solution accurately measures tissue collagen content. Tissue Eng Part C Methods 2017;23:243–50.

[36] Malla A, Lotersztajn S. Cellular mechanisms of tissue fibrosis. 5. Novel insights into liver fibrosis. Am J Physiol Cell Physiol 2013;305:C789–99.

[37] Botros M, Sikaris KA. The de ritis ratio: the test of time. Clin Biochem Rev 2013;34:117–30.

[38] Smejkalová J, Simek J, Rouchal J, Dvoráčková I. The time course of biochemical and histological changes following carbon tetrachloride-induced liver damage in rats of both sexes. Physiol Bohemoslov 1985;34:494–501.

[39] Watanabe T, Niioka M, Ishikawa A, Hozawa S, Arai M, Maruyama K, et al. Dynamic change of cells expressing MMP-2 mRNA and MT1-MMP mRNA in the recovery from liver fibrosis in the rat. J Hepatol 2001;35:465–73.

[40] Itaba N, Matsumi Y, Okinaka K, Ashla AA, Kono Y, Osaki M, et al. Human mesenchymal stem cell-engineered hepatic cell sheets accelerate liver regeneration in mice. Sci Rep 2015;5:16169.

[41] Itoh Y. Membrane-type matrix metalloproteinases: their functions and regulations. Matrix Biol 2015;44–46:207–23.

[42] Knäuper V, Bailey L, Worley JR, Soloway P, Patterson ML, Murphy G. Cellular activation of proMMP-13 by MT1-MMP depends on the C-terminal domain of MMP-13. FEBS Lett 2002;32:127–30.

[43] Will H, Atkinson SJ, Butler GS, Smith B, Murphy G. The soluble catalytic domain of membrane type 1 matrix metalloproteinase cleaves the propeptide of progelatinase A and initiates autoproteolytic activation. Regulation by TIMP-2 and TIMP-3. J Biol Chem 1996;271:17119–23.

[44] Shimizu H, Tsubota T, Kanki K, Shiota G. All-trans retinoic acid ameliorates hepatic stellate cell activation via suppression of thioredoxin interacting protein expression. J Cell Physiol 2018;233:607–16.

[45] Okuyama H, Nakamura H, Shimahara Y, Uyama N, Kwon YW, Kawada N, et al. Overexpression of thioredoxin prevents thioacetamide-induced hepatic fibrosis in mice. J Hepatol 2005;42:117–23.

[46] D'Ippolito G, Schiller PC, Ricordi C, Roos BA, Howard GA. Age-related osteogenic potential of mesenchymal stromal stem cells from human vertebral bone marrow. J Bone Miner Res 1999;14:1115–22.

[47] Zaim M, Karaman S, Cetin G, Isik S. Donor age and long-term culture affect differentiation and proliferation of human bone marrow mesenchymal stem cells. Ann Hematol 2012;91:1175–86.

[48] Lindsey ML, Goshorn DK, Squires CE, Escobar GP, Hendrick JW, Mingoia JT, et al. Age-dependent changes in myocardial matrix metalloproteinase/tissue inhibitor of metalloproteinase profiles and fibroblast function. Cardiovasc Res 2005;66:410–9.

[49] Lin J, Davis HB, Dai Q, Chou YM, Craig T, Hinojosa-Laborde C, et al. Effects of early and late chronic pressure overload on extracellular matrix remodeling. Hypertens Res 2008;31:1225–31.

[50] Memon IA, Sawa Y, Fukushima N, Matsumiya G, Miyagawa S, Taketani S, et al. Repair of impaired myocardium by means of implantation of engineered autologous myoblast sheets. J Thorac Cardiovasc Surg 2005;130:1333–41.

[51] Siltanen A, Nuutila K, Imanishi Y, Uenaka H, Makela J, Patila Y, et al. The paracrine effect of skeletal myoblasts is cardioprotective against oxidative stress and involves EGFR-ErbB4 signaling, cystathionase, and the unfolded protein response. Cell Transplant 2016;25:55–69.

[52] Iseoka H, Miyagawa S, Saito A, Harada A, Sawa Y. Role and therapeutic effects of skeletal muscle-derived non-myogenic cells in a rat myocardial infarction model. Stem Cell Res Ther 2020;11:69.